Adaptive finite time stabilization of chaotic flow with a single unstable node using a nonlinear function-based global sliding mode

Saleh Mobayen [a, *], Jun Ma [b], Gisela Pujol-Vazquez [c], Leonardo Acho [d], Quanmin Zhu [e]

[a] *Department of Electrical Engineering, Faculty of Engineering, University of Zanjan, Zanjan, Iran (mobayen@znu.ac.ir)*

[b] *Department of Physics, Lanzhou University of Technology, Lanzhou 730050, China (hyperchaos@163.com)*

[c] *Department of Mathematics, Universitat Politècnica de Catalunya-BarcelonaTech (ESEIAAT), Terrasa, Spain (gisela.pujol@upc.edu)*

[d] *Department of Mathematics, Universitat Politècnica de Catalunya-BarcelonaTech (EEBE), Barcelona, Spain (leonardo.acho@upc.edu)*

[e] *Department of Engineering Design and Mathematics, University of the West of England, Bristol, UK, Email (quan.zhu@uwe.ac.uk)*

Abstract: This article presents a novel adaptive finite time stabilization technique based on global sliding mode for disturbed chaotic flow with a single unstable node. The considered chaotic flow has unusual characteristics containing attractor merging, symmetry breaking, attracting tori and different forms of multi-stability. A nonlinear function is employed in the global sliding surface to modify damping ratio and improve the transient performance. The damping ratio of the closed-loop system is improved when the states converge to the origin. Using the new chattering-free controller, the reaching mode is removed and the sliding behavior is presented right from the first instant. The adaptive finite-time tuning law eliminates the requirement of the information about the disturbances' bounds. Illustrative simulations are provided to display the efficiency of the proposed scheme.

Keywords: Global sliding mode; adaptive gain tuning; finite-time control; chaotic flow; unstable node.

* Corresponding Author, E-mail address: mobayen@znu.ac.ir, url: http://www.znu.ac.ir/members/mobayen-saleh, Tel.: +98 24 3305 4219.

1. Introduction

Sliding mode control (SMC) is efficiently applied for the stabilization control of wide range of linear / nonlinear dynamic systems such as chaotic systems [1-4], power converters [5], singular systems [6], quad-rotor aircraft [7], inverted pendulum [8], seesaw systems [9], robotic manipulators [10], electronic circuits [11], power processing [12, 13], secure communication [14], vehicular following system [15], etc. SMC is a powerful control technique and has ability of achieving desirable performance in the presence of disturbances and uncertainties [16-18]. Of the important properties on SMC are the superior transient performance, insensitivity to the bounded disturbances and robustness to the uncertainties in comparison with the other control methods [19]. SMC design procedure is separated into these phases: (i) sliding phase, (ii) reaching phase. A switching surface is specified in the sliding phase so that the controlled system displays promising dynamic performance [20]. A sliding mode controller is used in the reaching phase to converge trajectories of the states to the switching surface [21]. For the purpose of the influence of the switching surface on the stabilization and transient response, the design procedure of the switching surface is the most significant subject [22, 23]. SMC uses a discontinuous control signal to drive the states to a predesigned sliding surface on which the desired performance and system's stability are achieved [24]. However, SMC cannot fulfill the convergence of the state trajectories to zero in the finite time. In reality, particularly in some engineering aspects, it is required that the convergence of the dynamical system is obtained in the finite time rather than infinite time [25, 26]. The problem of finite time control has been investigated by quite a few researchers from different viewpoints [27]. Through the reaching phase of SMC, the system doesn't have the robust performance, and the parametric uncertainties and external disturbances can destabilize the control system.

In the past years, the theory of global sliding mode control (GSMC) has been presented for a general framework to remove the reaching period of SMC and overcome undesired chattering phenomenon. In GSMC, via an extra term in the surface, the reaching mode is removed and the states of the control system move on the sliding surface right from the initial instant. In recent decade, more attention has been paid for the use of GSMC method [28]. In [29], a GSMC scheme is offered for the stabilization control of a helicopter with disturbance and input-delay. A fuzzy GSMC based on backstepping is proposed in [30] for tracking control of multi-joint robotic manipulators. The problem of network congestion control based on GSMC and linear matrix inequality (LMI) is studied in [31] for TCP network systems with state-delays and external disturbances. In [32], a global quasi-SMC technique is investigated to ensure zigzag motion with small bound throughout the entire response for the achievement of disturbance rejection in discrete time. In [33], the design problem of adaptive GSMC is studied for linear helicopter systems with actuator fault and time-delay. The adaptive fast terminal sliding mode (FTSM) control method joined with GSMC scheme is planned in [34] for tracking control of the uncertain nonlinear third-order systems. In [35], an adaptive GSMC via radial basis function (RBF) neural-network is offered for the identification purpose and tracker design of micro-electro-mechanical system (MEMS) gyroscope. A novel GSMC technique based on LMI and Lyapunov stability theory is studied in [36] for the stabilization control of uncertain nonlinear dynamic systems with perturbation. In [37], an adaptive global nonlinear switching surface is proposed for the nonlinear dynamic systems with external disturbances. In [38], an LMI-based GSMC law is suggested to improve the stability and robustness of the underactuated systems with external disturbances. In [39], a dynamic proportional-integral-derivative (PID) GSMC based on an adaptive RBF neural estimator is developed to satisfy the stability and robustness of MEMS gyroscope. An adaptive super-twisting GSMC is proposed in [40] for the tracking control of n-link rigid robotic manipulators. In order to improve the control

performance of GSMC, a fast GSMC technique is presented in [41] to accelerate the system response by changing the exponential decay function to an exponential bilateral decay function.

In this article, an adaptive GSMC method is investigated to remove the reaching phase and overcome the chattering phenomenon. In the presence of the nonlinear function ψ in the global sliding surface, the damping ratio of the chaotic flow with external disturbance is improved and the robustness of the chaotic flow is enhanced. Besides, an adaptation process is used in GSMC which approximates the disturbances' unknown upper bounds and satisfies the finite time convergence of state trajectories to the global sliding surface. As a final point, some numerical simulations on chaotic flow with a single unstable node are provided to validate the efficiency of the suggested approach. The main purpose of this article is to propose an adaptive GSMC framework to stabilize the chaotic systems in the existence of external disturbances with unknown bounds.

The organization of this article is formed as follows: Section 2 covers the problem description of the chaotic flow with a single unstable node. Section 3 presents the design approach of the adaptive finite time stabilizer using global sliding mode scheme. In Section 4, the designed adaptive finite time stabilization technique is employed on the disturbed chaotic flow in comparison with the other techniques. Finally, in Section 5, conclusions are drawn.

2. System description

A modified jerk system is studied, as the simplest chaotic flow with a single unstable node, using a form that has successfully given other chaotic flows with hidden attractors (see references [42] and [42] for more details). The chaotic flows with hidden attractors are significant and potentially problematic in engineering applications [43-45].

Consider the chaotic flow with single unstable node described as [42]

$$\begin{aligned}\dot{x}_1 &= x_2,\\ \dot{x}_2 &= -x_1 + x_2x_3 + u_1 + d_1,\\ \dot{x}_3 &= x_3 + ax_1^{\,2} - x_2^{\,2} - b + u_2 + d_2,\end{aligned} \tag{1}$$

where $x=[x_1, x_2, x_3]^T$, $u=[u_1, u_2]^T$ and $d=[d_1, d_2]^T$ denote the states of the system, control signals, and external disturbances, respectively. The chaotic flow (1) can be represented as

$$\begin{aligned}\dot{x}_1 &= A_{11}x_1 + A_{12}z,\\ \dot{z} &= A_{21}x_1 + A_{22}z + Bu + Bf(x_1, z) + d,\end{aligned} \tag{2}$$

where $z=\begin{bmatrix}x_2 & x_3\end{bmatrix}^T$, $f(x_1,z)=\begin{bmatrix} x_2x_3 \\ ax_1^{\,2} - x_2^{\,2} - b\end{bmatrix}$, $A_{11}=0$, $A_{12}=\begin{bmatrix}1 & 0\end{bmatrix}$, $B=\begin{bmatrix}1\\1\end{bmatrix}$, $A_{21}=\begin{bmatrix}-1\\0\end{bmatrix}$, $A_{22}=\begin{bmatrix}0 & 0\\0 & 1\end{bmatrix}$.

Assumption 1: Assume $\bar{A}=\begin{bmatrix}A_{11} & A_{12}\\A_{21} & A_{22}\end{bmatrix}$ and $\bar{B}=[0 \;\; B^T]^T$. The pair $(\bar{A}, \bar{B})$ is completely controllable; because the determinant of the controllability matrix $\bar{P}=\left[\bar{B}\,\middle|\,\bar{A}\bar{B}\,\middle|\,\bar{A}^2\bar{B}\right]=\begin{bmatrix}0 & 1 & 0\\1 & 0 & -1\\1 & 1 & 1\end{bmatrix}$ is $\left|\bar{P}\right|=-2\neq 0$.

Hence, it is obtained from (2) that the pair (A_{11}, A_{12}) is controllable. Therefore, for any positive constant w, there exists a unique positive scalar p as the solution of the Lyapunov condition $A_{12}F = w/(2p)$, where $F=[F_1 \;\; F_2]^T$ is a constant gain vector.

3. Main results

The global switching surface for chaotic flow (2) is chosen by

$$\sigma = \Gamma\left(x - Hx_0\right), \tag{3}$$

with

$$\Gamma = \left[F - p\psi(x_1(t))A_{12}^T \quad I_2 \right], \tag{4}$$

where x_0 is the initial condition of x; I_2 is two-dimensional identity matrix; p denotes a positive scalar; F is a constant gain vector; $\psi(x_1(t))$ is a diagonal matrix with non-positive nonlinear scalar functions of $x_1(t)$, and $H = \text{diag}[\exp(-\beta_1 t), \exp(-\beta_2 t), \exp(-\beta_3 t)]$, where $\beta_1, \beta_2, \beta_3$ are positive constants. The subsequent inequality is obtained for some positive constants ρ and q

$$\|H\| \le q \exp(-\rho t). \tag{5}$$

The nonlinear function $\psi(x_1(t))$ is selected in the form of a diagonal matrix with exponential terms as

$$\psi(x_1(t)) = diag[\psi_1(x_1(t)), \psi_2(x_1(t))], \tag{6}$$

$$\psi_i(x_1(t)) = -\mu_i \exp\left(-\delta_i \frac{\|x_1(t)\|}{t} \right), \tag{7}$$

where μ_i and δ_i are positive constants. The function $\psi_i(x_1(t))$ varies its value from zero to $-\mu_i$ while the state $x(t)$ converges to zero from the initial value, with $\psi_i(x_1(t_0)) = \psi_i(x_1(0)) = 0$. From now, we denote $\psi_1(x_1(t))$ as ψ_1.

On the sliding surface $\sigma = 0$, one can attain from (3) that

$$\begin{aligned} x_2 &= (p\psi_1 - F_1)(x_1 - \exp(-\beta_1 t)x_{10}) + \exp(-\beta_2 t)x_{20}, \\ x_3 &= -F_2(x_1 - \exp(-\beta_1 t)x_{10}) + \exp(-\beta_3 t)x_{30}, \end{aligned} \tag{8}$$

where x_{i0} is the initial condition of x_i. Substituting x_2 from (8) into the first equation of chaotic flow (2), one achieves

$$\dot{x}_1(t) = \left(p\psi_1 - F_1 \right)\left(x_1 - \exp(-\beta_1 t)x_{10} \right) + \exp(-\beta_2 t)x_{20}. \tag{9}$$

Theorem 1: Consider the dynamics (9) and suppose Assumption 1 fulfilled. As a result, the state $x_1(t)$ of the sliding mode dynamics (9) converges to zero, exponentially.

Proof: Define the Lyapunov candidate functional as

$$V_a = 0.5 p x_1^{\,2}. \tag{10}$$

Differentiating (10) along trajectories of (9) yields

$$\begin{aligned} \dot{V}_a &= p x_1 \dot{x}_1 \\ &= p x_1 \left(\left(p\psi_1 - F_1 \right) \left(x_1 - \exp(-\beta_1 t) x_{10} \right) + \exp(-\beta_2 t) x_{20} \right) \end{aligned} \tag{11}$$

The infinite limit of H is found as

$$\lim_{t\to\infty} H = \lim_{t\to\infty} \left(\text{diag}[\, e^{-\beta_1 t},\, e^{-\beta_2 t}, e^{-\beta_3 t}\,] \right) = 0, \tag{12}$$

and using the Lyapunov criterion $A_{12} F = w/(2p)$, we can obtain from (11) that

$$\begin{aligned} \dot{V}_a &= p\left(p\psi_1 - F_1 \right) x_1^{\,2} \\ &= p^2 \psi_1 x_1^{\,2} - 0.5 w x_1^{\,2}. \end{aligned} \tag{13}$$

Because $\psi_1 < 0$ and $w > 0$, then Eq. (13) is found as

$$\dot{V}_a \le -0.5 w x_1^{\,2} \le -\alpha_1 V_a < 0, \tag{14}$$

with $\alpha_1 = w/p$.

Theorem 2: Consider the disturbed chaotic flow (2) with a single unstable node. Applying the control inputs as

$$\begin{aligned} u_1 &= -k_1 \sigma_1 - k_2 \,\text{sgn}(\sigma_1) + \dot{\psi}_1 p \left(x_1 - \exp(-\beta_1 t) x_{10} \right) \\ &\quad - (F_1 - p\psi_1) \left(x_2 + \beta_1 \exp(-\beta_1 t) x_{10} \right) + x_1 - x_2 x_3 - \beta_2 \exp(-\beta_2 t) x_{20}, \end{aligned} \tag{15}$$

$$\begin{aligned} u_2 &= -k_1 \sigma_2 - k_3 \,\text{sgn}(\sigma_2) \\ &\quad - F_2 \left(x_2 + \beta_1 \exp(-\beta_1 t) x_{10} \right) - x_3 - a x_1^{\,2} + x_2^{\,2} + b - \beta_3 \exp(-\beta_3 t) x_{30}, \end{aligned} \tag{16}$$

where $\sigma_1 = x_2 - \exp(-\beta_2 t)x_{20} + (F_1 - p\psi_1)(x_1 - \exp(-\beta_1 t)x_{10})$, $\sigma_2 = F_2(x_1 - \exp(-\beta_1 t)x_{10}) + x_3 - \exp(-\beta_3 t)x_{30}$, $k_1 > 0$, $k_2 > |d_1|$, $k_3 > |d_2|$, then, the states of the chaotic flow (2) are moved from initial conditions to the global surface (3) in the finite time and stay on the surface forever.

Proof: Describe the Lyapunov candidate functional as

$$V_b = 0.5\sigma^T\sigma. \tag{17}$$

Time-derivative of V_b along states of the chaotic flow (1) is calculated as

$$\begin{aligned}\dot{V}_b &= \sigma^T\dot{\sigma}\\ &= \sigma^T\left(\dot{\Gamma}(x - Hx_0) + \Gamma(\dot{x} - \dot{H}x_0)\right)\\ &= \sigma^T\begin{pmatrix} -\dot{\psi}_1 p(x_1 - \exp(-\beta_1 t)x_{10}) + (F_1 - p\psi_1)(x_2 + \beta_1\exp(-\beta_1 t)x_{10}) - x_1 + x_2x_3 + u_1 + d_1 + \beta_2\exp(-\beta_2 t)x_{20} \\ F_2(x_2 + \beta_1\exp(-\beta_1 t)x_{10}) + x_3 + ax_1^{\,2} - x_2^{\,2} - b + u_2 + d_2 + \beta_3\exp(-\beta_3 t)x_{30}\end{pmatrix}.\end{aligned} \tag{18}$$

Substituting (15) and (16) into (18), we achieve

$$\begin{aligned}\dot{V}_b &= \sigma^T\begin{pmatrix} d_1 - k_1\sigma_1 - k_2\,\mathrm{sgn}(\sigma_1) \\ d_2 - k_1\sigma_2 - k_3\,\mathrm{sgn}(\sigma_2)\end{pmatrix}\\ &= d_1\sigma_1 - k_1\sigma_1^{\,2} - k_2|\sigma_1| + d_2\sigma_2 - k_1\sigma_2^{\,2} - k_3|\sigma_2|\\ &\le |d_1||\sigma_1| - k_2|\sigma_1| - k_1\sigma_1^{\,2} - k_1\sigma_2^{\,2} + |d_2||\sigma_2| - k_3|\sigma_2|\\ &\le -k_1\sigma_1^{\,2} - k_1\sigma_2^{\,2}\\ &= -2k_1V_b < 0.\end{aligned} \tag{19}$$

Hence, the states of the disturbed chaotic flow (1) are converged to the global surface $\sigma = 0$ in the finite time and after that, stay on it. □

In practice, the upper bounds of the disturbance terms d_1 and d_2 are unknown. In the following theorem, the adaptive gain tuning laws are planned to estimate the unknown bounds of the external disturbances.

Theorem 3: Consider the disturbed chaotic flow (2) and the global switching surface (3). Suppose that the external disturbances are unknown but bounded, that is, $k_2 > |d_1|$ and $k_3 > |d_2|$, where k_2 and k_3 are

unknown positive scalars. Assume that $\hat{k}_2$ and $\hat{k}_3$ are the estimation values of k_2 and k_3 which are provided by the adaptive gain tuning laws as

$$\dot{\hat{k}}_2 = \kappa_2 |\sigma_1|, \tag{20}$$

$$\dot{\hat{k}}_3 = \kappa_3 |\sigma_2|, \tag{21}$$

where κ_2 and κ_3 are two positive constants. Applying the adaptive controllers as

$$\begin{aligned} u_1 = & -k_1\sigma_1 - \hat{k}_2 \operatorname{sgn}(\sigma_1) + \dot{\psi}_1 p \left(x_1 - \exp(-\beta_1 t)x_{10}\right) - x_2 x_3 \\ & + x_1 - (F_1 - p\psi_1)\left(x_2 + \beta_1 \exp(-\beta_1 t)x_{10}\right) - \beta_2 \exp(-\beta_2 t)x_{20}, \end{aligned} \tag{22}$$

$$\begin{aligned} u_2 = & -k_1\sigma_2 - \hat{k}_3 \operatorname{sgn}(\sigma_2) - x_3 - \alpha {x_1}^2 + {x_2}^2 + b \\ & - F_2\left(x_2 + \beta_1 \exp(-\beta_1 t)x_{10}\right) - \beta_3 \exp(-\beta_3 t)x_{30}, \end{aligned} \tag{23}$$

then, the finite-time convergence of the states of disturbed chaotic flow (2) to the sliding surface $\sigma = 0$ is satisfied.

Proof: The Lyapunov candidate functional is described by

$$V_c = 0.5\left(\sigma^T\sigma + \gamma_1 \tilde{k}_2^{\,2} + \gamma_2 \tilde{k}_3^{\,2}\right), \tag{24}$$

with $\tilde{k}_2 = \hat{k}_2 - k_2$ and $\tilde{k}_3 = \hat{k}_3 - k_3$. Calculating the time derivative of (24) gives

$$\begin{aligned} \dot{V}_c &= \sigma^T\dot{\sigma} + \gamma_1 \tilde{k}_2 \dot{\tilde{k}}_2 + \gamma_2 \tilde{k}_3 \dot{\tilde{k}}_3 \\ &= \sigma^T\left(\dot{\Gamma}\left(x - Hx_0\right) + \Gamma\left(\dot{x} - \dot{H}x_0\right)\right) + \gamma_1\left(\hat{k}_2 - k_2\right)\dot{\hat{k}}_2 + \gamma_2\left(\hat{k}_3 - k_3\right)\dot{\hat{k}}_3. \end{aligned} \tag{25}$$

where substituting (20)-(23) in (25), we have

$$
\begin{aligned}
\dot{V}_c &= \begin{bmatrix}\sigma_1 & \sigma_2\end{bmatrix}\begin{pmatrix} d_1 - k_1\sigma_1 - \hat{k}_2\,\mathrm{sgn}(\sigma_1) \\ d_2 - k_1\sigma_2 - \hat{k}_3\,\mathrm{sgn}(\sigma_2)\end{pmatrix} + \gamma_1\kappa_2\left(\hat{k}_2 - k_2\right)|\sigma_1| + \gamma_2\kappa_3\left(\hat{k}_3 - k_3\right)|\sigma_2| \\
&= d_1\sigma_1 - k_1{\sigma_1}^2 - \hat{k}_2|\sigma_1| + d_2\sigma_2 - k_1{\sigma_2}^2 - \hat{k}_3|\sigma_2| + \gamma_1\kappa_2\tilde{k}_2|\sigma_1| + \gamma_2\kappa_3\tilde{k}_3|\sigma_2| \\
&\le |d_1||\sigma_1| - \hat{k}_2|\sigma_1| + \gamma_1\kappa_2\tilde{k}_2|\sigma_1| + k_2|\sigma_1| - k_2|\sigma_1| \\
&\quad + |d_2||\sigma_2| - \hat{k}_3|\sigma_2| + \gamma_2\kappa_3\tilde{k}_3|\sigma_2| + k_3|\sigma_2| - k_3|\sigma_2| \\
&\le -\left(k_2 - |d_1|\right)|\sigma_1| - \left(1 - \gamma_1\kappa_2\right)\tilde{k}_2|\sigma_1| - \left(k_3 - |d_2|\right)|\sigma_2| - \left(1 - \gamma_2\kappa_3\right)\tilde{k}_3|\sigma_2|
\end{aligned}
\tag{26}
$$

Since $k_2 > |d_1|$, $k_3 > |d_2|$, $\gamma_1\kappa_2 < 1$ and $\gamma_2\kappa_3 < 1$, then we obtain from (26) that

$$
\begin{aligned}
\dot{V}_c &\le -\left(k_2 - |d_1|\right)|\sigma_1| - \left(1 - \gamma_1\kappa_2\right)\tilde{k}_2|\sigma_1| \\
&\quad - \left(k_3 - |d_2|\right)|\sigma_2| - \left(1 - \gamma_2\kappa_3\right)\tilde{k}_3|\sigma_2| \\
&\le -\sqrt{2}\left(k_2 - |d_1|\right)|\sigma_1|/\sqrt{2} - \sqrt{2/\gamma_1}\left(1 - \gamma_1\kappa_2\right)|\sigma_1|\left(\tilde{k}_2/\sqrt{2/\gamma_1}\right) \\
&\quad - \sqrt{2}\left(k_3 - |d_2|\right)|\sigma_2|/\sqrt{2} - \sqrt{2/\gamma_2}\left(1 - \gamma_2\kappa_3\right)|\sigma_2|\left(\tilde{k}_3/\sqrt{2/\gamma_2}\right) \\
&\le -\min\left(\sqrt{2}\left(k_2 - |d_1|\right), \sqrt{2}\left(k_3 - |d_2|\right), \sqrt{2/\gamma_1}\left(1 - \gamma_1\kappa_2\right)|\sigma_1|, \sqrt{2/\gamma_2}\left(1 - \gamma_2\kappa_3\right)|\sigma_2|\right) \\
&\quad \times \left(\left(|\sigma_1| + |\sigma_2|\right)/\sqrt{2} + \tilde{k}_2/\sqrt{2/\gamma_1} + \tilde{k}_3/\sqrt{2/\gamma_2}\right) \\
&\le -\aleph {V_c}^{0.5}.
\end{aligned}
\tag{27}
$$

where $\aleph = \min\left(\sqrt{2}\left(k_2 - |d_1|\right), \sqrt{2}\left(k_3 - |d_2|\right), \sqrt{2/\gamma_1}\left(1 - \gamma_1\kappa_2\right)|\sigma_1|, \sqrt{2/\gamma_2}\left(1 - \gamma_2\kappa_3\right)|\sigma_2|\right) > 0$. Thus, the states of the disturbed chaotic flow (2) are converged to the global switching surface $\sigma = 0$ in the finite time. □

4. Simulation results

In what follows, to specify the effectiveness of the scheme, to conduct simulation tests in comparison with the method of [1]. Consider the chaotic flow having a single unstable node [42] with some changes as

$$
\begin{aligned}
\dot{x}_1 &= x_2, \\
\dot{x}_2 &= -x_1 + x_2x_3 + u_1 + d_1, \\
\dot{x}_3 &= x_3 + 8.894{x_1}^2 - {x_2}^2 - 4 + u_2 + d_2,
\end{aligned}
\tag{28}
$$

where $d_1 = 0.3\cos(3x_1) - 0.4\sin(2x_1x_2)$ and $d_2 = 0.2\sin(2x_2x_3) + 0.3\cos(2x_1)$. The modified system (27) includes external disturbances d_1 and d_2, and control laws u_1 and u_2 to stabilize it in finite time. The

system proposed in [42] has a chaotic behavior in a wide parameter range. As shown in Fig. 1, the orbits of the states for the uncontrolled chaotic flow display chaotic behavior and clear sensitivity to initial conditions. This system demonstrates strange double-scroll attractors as illustrated in Fig. 2.

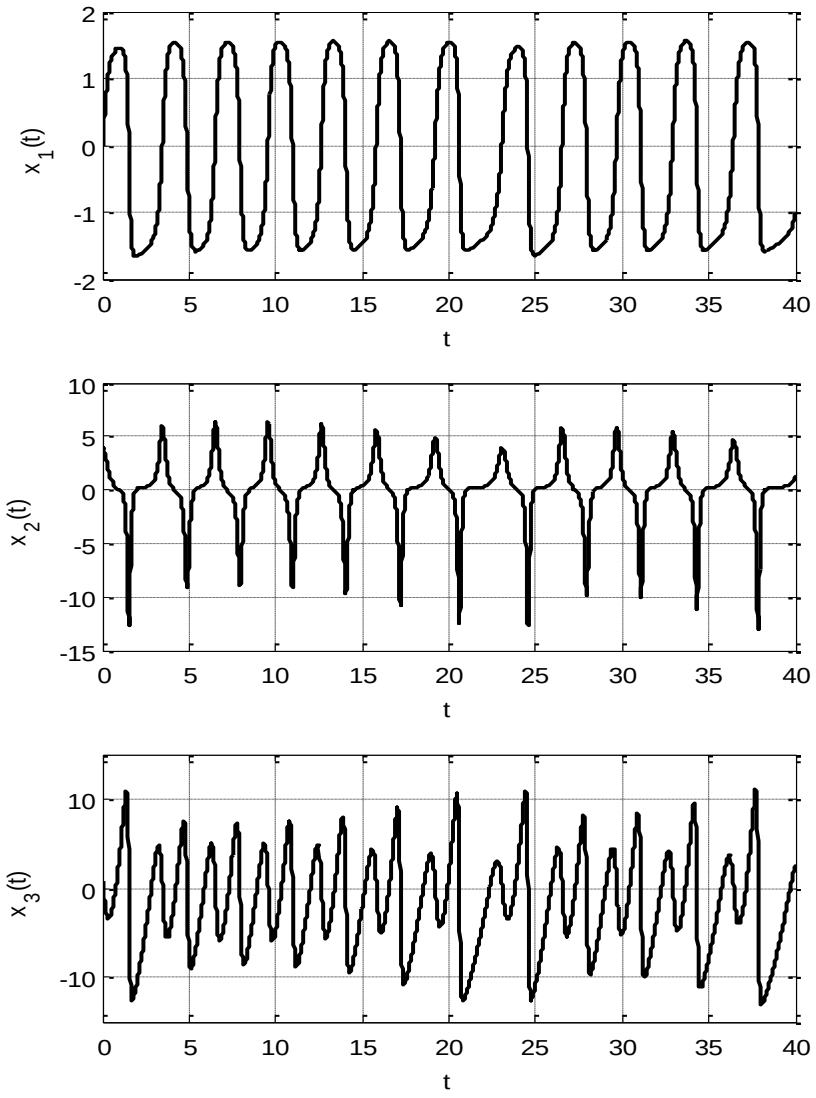

Fig. 1. Chaotic response of the uncontrolled chaotic flow.

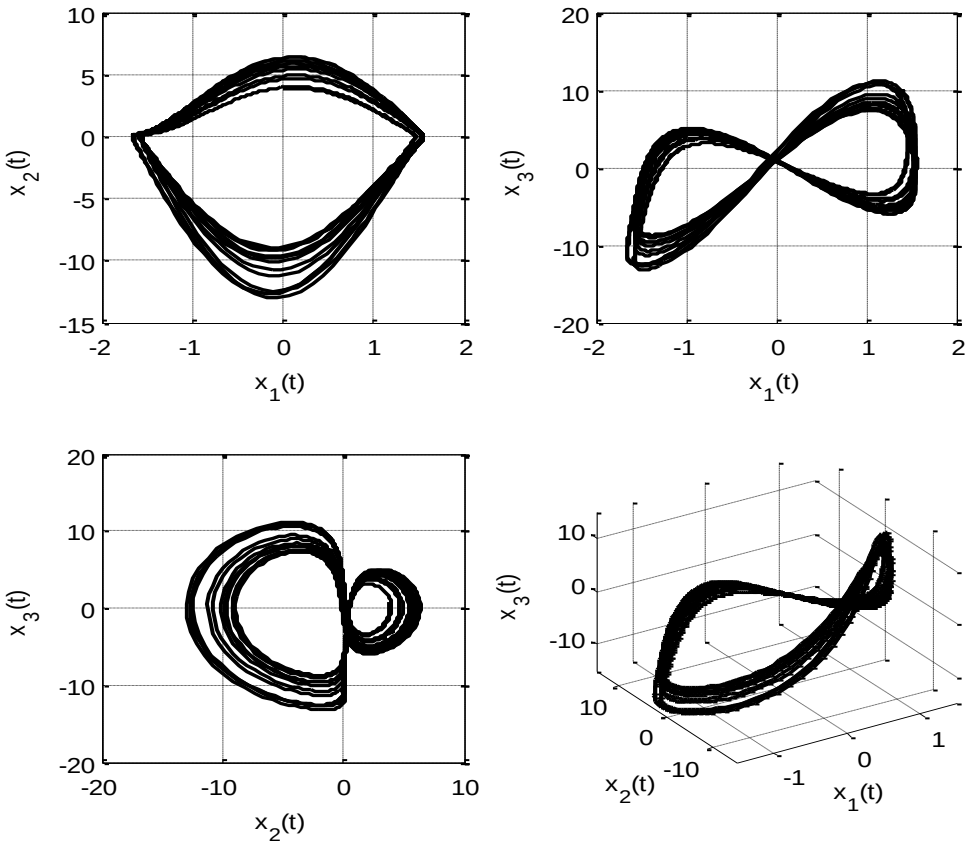

Fig. 2. Chaotic attractors for $a = 8.894,\ b = 4$.

Simulation results are performed via Matlab® software. The initial states are chosen as $\hat{k}_2(0) = 0.5$, $\hat{k}_3(0) = 0$, $x(0) = [0 \quad 3.8 \quad 0.7]^T$. The constant parameters are chosen as $\kappa_2 = 0.4$, $\kappa_3 = 0.3$, $k_1 = 2$, $\beta_1 = 1$, $\beta_2 = 2$, $\beta_3 = 3$, $\mu_1 = 20$, $\delta_1 = 2$ and $F = [0.8 \quad 0.4]^T$. By solving the Lyapunov function $A_{12}F = w/(2p)$ for $w = 2$, one obtains $p = 1.25$. Fig.3 illustrates the time histories of the states of the chaotic flow. According to the inequality (27), finite time period can be calculated as follows:

By dividing two sides of $\dot{V}_c \le -\aleph V_c^{0.5}$ (Eq. (27)) to term $V_c^{0.5}$, one achieves $V_c^{-0.5}\dot{V}_c \le -\aleph$, where after some calculations, it yields $dt \le -\aleph^{-1} V_c^{-0.5} dV_c$. Now, using integration from t_0 to t_s, one attains $t_s - t_0 \le \frac{2}{\aleph} V_c(0)^{0.5}$. Hence, finite time period is obtained as $t_s = t_0 + \frac{2}{\aleph}\sqrt{V_c(0)}$. The settling times of the

proposed controller, linear sliding surface (without the nonlinear function $\psi(x)$**)** and the method of [1] are calculated for $x_1(t)$ as 1.493 *s*, 2.177 *s* and 6.2915 *s*; for $x_2(t)$ as 1.04 *s*, 2.047 *s* and 4.366 *s*; for $x_3(t)$ as 0.893 *s*, 1.904 *s* and 5.63 *s*, respectively. It is demonstrated that the states converge to the origin quickly compared with the results of the linear sliding surface (without the nonlinear function $\psi(x)$**)** and the method of [1]. It is an obvious evidence from Fig.3 that the settling-time and overshoot of the system states decrease noticeably using the proposed control approach. Thus, the presence of the nonlinear function $\psi(x_1)$ helps for the improvement of the value of damping ratio.

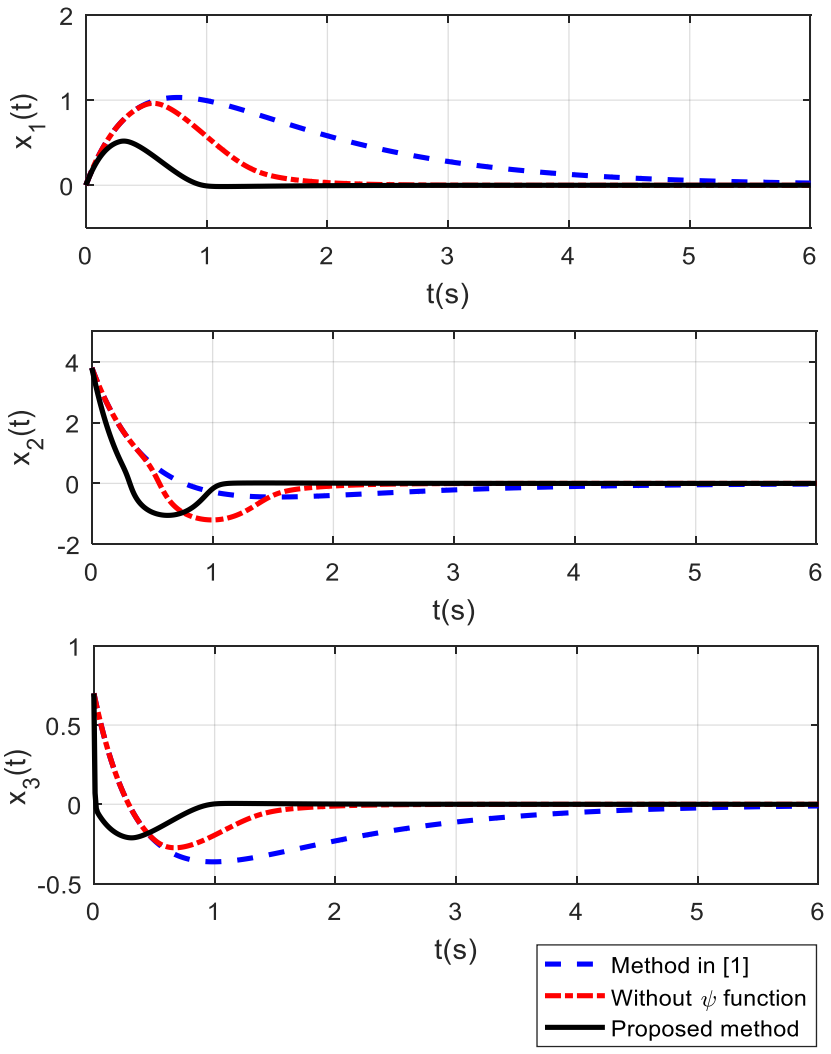

Fig.3. State histories of the chaotic flow.

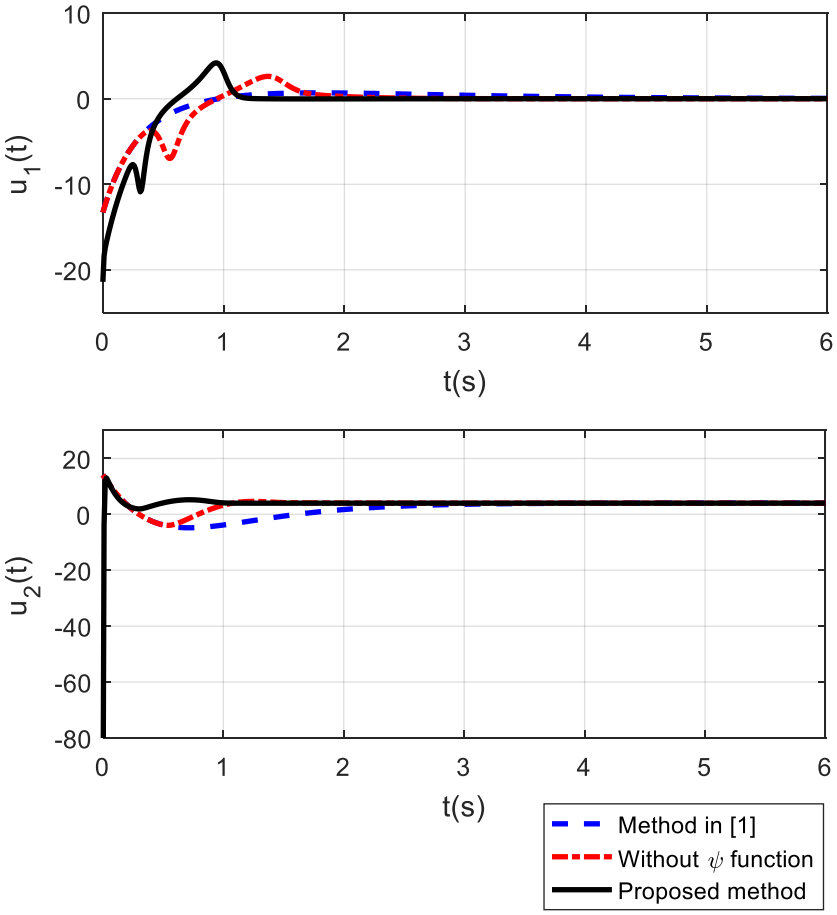

Fig.4. Time histories of the control inputs.

Inspection of time trajectories of the control inputs in Fig.4, it is obvious that the recommended controllers produce faster responses than the results of the other methods. Time histories of the global sliding surfaces are plotted in Fig.5, which demonstrates that the surfaces approach to the origin in the finite time. It i observed from Fig.5 that the GSMC surfaces start from zero and the reaching phase is removed. Hence, the robustness of the system to the external disturbances is satisfied right from the beginning of the entire response.

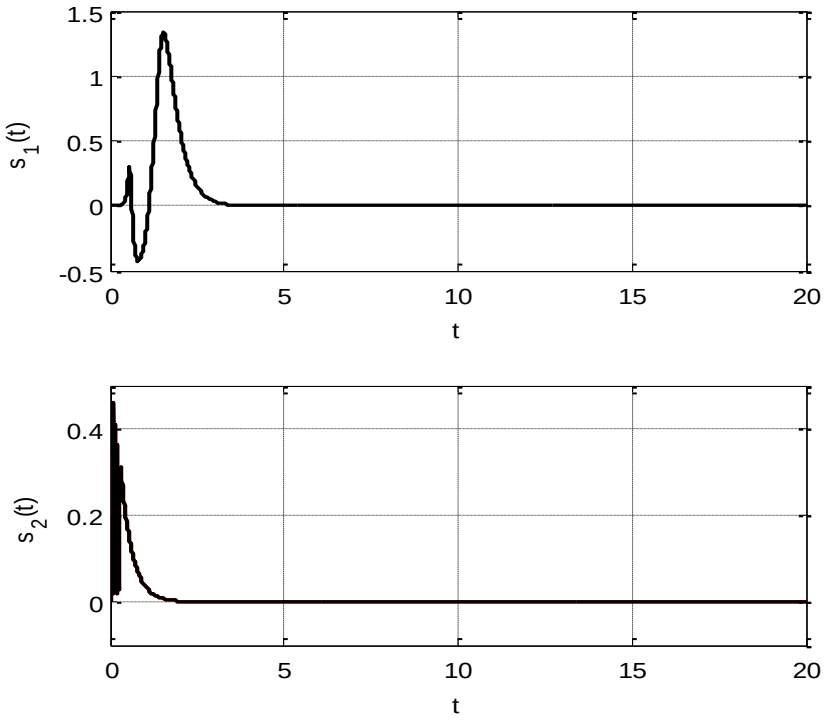

Fig.5. Time trajectories of the global surfaces.

Variations of the nonlinear function $\psi_1(x_1)$ and system's eigenvalue λ are presented in Fig.6. It is obvious from Fig.6 that the value of the nonlinear function $\psi_1(x_1)$ decreases from zero to negative high amount as the norm of the states converges to zero. Time trajectories of the adaptive gains $\hat{k}_2$ and $\hat{k}_3$ are shown in Fig.7. The obtained values for the adaptive gains are $\hat{k}_2 = 0.96$ and $\hat{k}_3 = 0.67$. Simulation results indicate the success of the planned control technique compared to the control signal without nonlinear function $\psi(x)$ and the control method of [1].

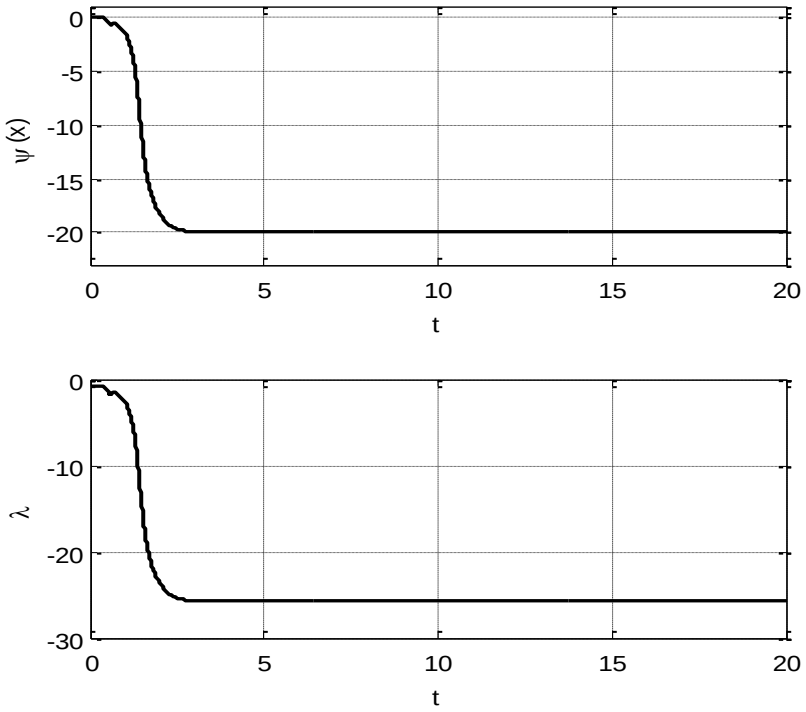

Fig.6. Variations of the nonlinear function $\psi_1(x)$ and eigenvalue λ.

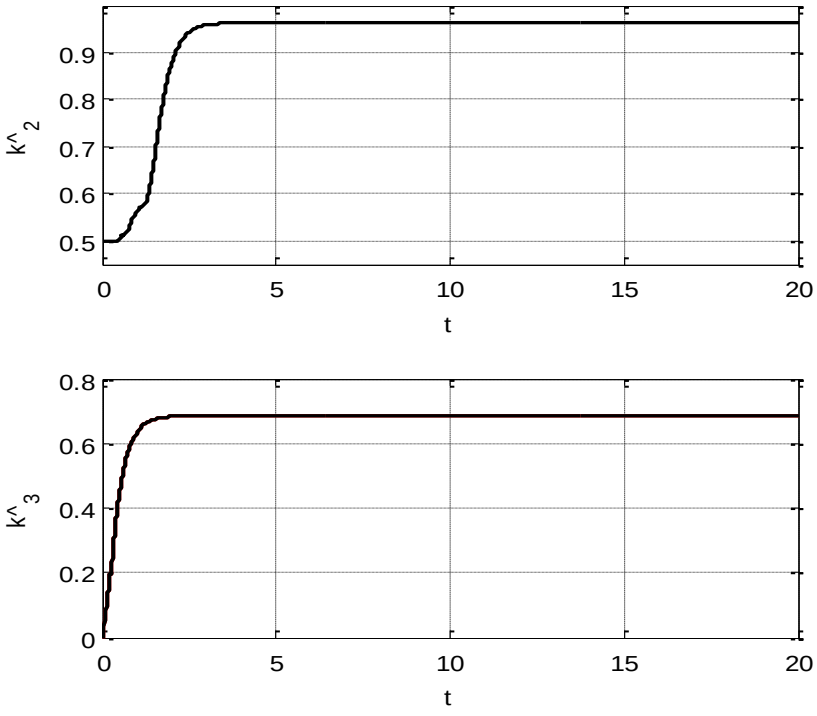

Fig.7. Time histories of the adaptive gains.

5. Conclusions

This article proposes a new adaptive finite-time stabilization method based on global sliding mode to advance the steady-state and transient performances of a class of chaotic flows in the presence of disturbances. The considered chaotic flow is an unusual model of a three-dimensional dissipative chaotic flow with a single unstable node. Using the nonlinear function in the global switching surface, the damping ratio of the overall system is bettered and the fast settling-time and small control signals are obtained. The proposed control scheme fulfills the robustness in contrast to the nonlinearities and disturbances, and also removes the chattering phenomenon and reaching mode. The global sliding mode is designed to form a switching surface for deletion of the reaching interval. The designed adaptive controller is used for the removal of the effects of the nonlinearities and disturbances, and also satisfied the finite time convergence to the defined global sliding surface. Lastly, a chaotic flow with a single unstable node exhibits the efficiency of the proposed method in comparison with the method of [1]. The further studies in this aspect can be extended to neuron networks via the results stated in [46, 47].

6. Acknowledgements

This work was partially supported by the Spanish Ministry of Economy, Industry and Competitiveness, under grants DPI2016-77407-P (AEI/FEDER, UE) and DPI2015-64170-R (MINECO/FEDER).

References

1. Zhang X, Liu X, Zhu Q. Adaptive chatter free sliding mode control for a class of uncertain chaotic systems. Applied Mathematics and Computation. 2014;232:431-5.
2. Mobayen S, Baleanu D, Tchier F. Second-order fast terminal sliding mode control design based on LMI for a class of non-linear uncertain systems and its application to chaotic systems. Journal of Vibration and Control. 2016;23(18):2912-25.
3. Martinez-Guerra R, Yu W. Chaotic synchronization and secure communication via sliding-mode observer. International Journal of Bifurcation and Chaos. 2008;18(01):235-43.
4. Sangpet T, Kuntanapreeda S. Output feedback control of unified chaotic systems based on feedback passivity. International Journal of Bifurcation and Chaos. 2010;20(05):1519-25.
5. Bai J, Lu SQ, Liu J. Study and Application of Sliding Mode Control Strategy for High-Power Current Source Inverter. Applied Mechanics and Materials. 2014;527:259-66.

6. Jiang B, Gao C, Xie J. Passivity based sliding mode control of uncertain singular Markovian jump systems with time-varying delay and nonlinear perturbations. Applied Mathematics and Computation. 2015;271:187-200.
7. González I, Salazar S, Lozano R. Chattering-free sliding mode altitude control for a quad-rotor aircraft: Real-time application. Journal of Intelligent & Robotic Systems. 2014;73(1-4):137-55.
8. LI X-B, MA L, DING S-H. A new second-order sliding mode control and its application to inverted pendulum. Acta Automatica Sinica. 2015;1:022.
9. Tsai C-H, Chung H-Y, Yu F-M. Neuro-sliding mode control with its applications to seesaw systems. IEEE Transactions on Neural Networks. 2004;15(1):124-34.
10. Van M, Kang H-J, Shin K-S. Backstepping quasi-continuous high-order sliding mode control for a Takagi–Sugeno fuzzy system with an application for a two-link robot control. Proceedings of the Institution of Mechanical Engineers, Part C: Journal of Mechanical Engineering Science. 2014;228(9):1488-500.
11. Zhao X, Yang H, Zong G. Adaptive Neural Hierarchical Sliding Mode Control of Nonstrict-Feedback Nonlinear Systems and an Application to Electronic Circuits. IEEE Transactions on Systems, Man, and Cybernetics: Systems. 2017;47(7):1394-404.
12. Cid-Pastor A, Martinez-Salamero L, El Aroudi A, Giral R, Calvente J, Leyva R. Synthesis of loss-free resistors based on sliding-mode control and its applications in power processing. Control Engineering Practice. 2013;21(5):689-99.
13. Ni J, Liu L, Liu C, Hu X, Li S. Fast fixed-time nonsingular terminal sliding mode control and its application to chaos suppression in power system. IEEE Transactions on Circuits and Systems II: Express Briefs. 2017;64(2):151-5.
14. Chen C-K, Yan J-J, Liao T-L. Sliding mode control for synchronization of Rössler systems with time delays and its application to secure communication. Physica Scripta. 2007;76(5):436.
15. Li S-B, Li K-Q, Wang J-Q, Yang B. Nonsingular fast terminal-sliding-mode control method and its application on vehicular following system. Control Theory & Applications. 2010;5:004.
16. Li P, Ma J, Zheng Z. Robust adaptive sliding mode control for uncertain nonlinear MIMO system with guaranteed steady state tracking error bounds. Journal of the Franklin Institute. 2016;353(2):303-21.
17. Wu L, Mazumder SK, Kaynak O. Sliding Mode Control and Observation for Complex Industrial Systems—Part II. IEEE Transactions on Industrial Electronics. 2018;65(1):830-3.
18. Jeong S, Chwa D. Coupled Multiple Sliding-Mode Control for Robust Trajectory Tracking of Hovercraft With External Disturbances. IEEE Transactions on Industrial Electronics. 2018;65(5):4103-13.
19. Nasiri A, Nguang SK, Swain A. Adaptive sliding mode control for a class of MIMO nonlinear systems with uncertainties. Journal of the Franklin Institute. 2014;351(4):2048-61.
20. Polyakov A, Fridman L. Stability notions and Lyapunov functions for sliding mode control systems. Journal of the Franklin Institute. 2014;351(4):1831-65.
21. Wang B, Shi P, Karimi HR. Fuzzy sliding mode control design for a class of disturbed systems. Journal of the Franklin Institute. 2014;351(7):3593-609.
22. Yang J, Li S, Yu X. Sliding-mode control for systems with mismatched uncertainties via a disturbance observer. IEEE Transactions on industrial electronics. 2013;60(1):160-9.
23. Li H, Yu J, Hilton C, Liu H. Adaptive sliding-mode control for nonlinear active suspension vehicle systems using T–S fuzzy approach. IEEE Transactions on Industrial Electronics. 2013;60(8):3328-38.
24. Barambones O, Alkorta P. A robust vector control for induction motor drives with an adaptive sliding-mode control law. Journal of the Franklin Institute. 2011;348(2):300-14.
25. Xu Y, Meng D, Xie C, You G, Zhou W. A class of fast fixed-time synchronization control for the delayed neural network. Journal of the Franklin Institute. 2018;355(1):164-76.
26. Xu Y, Ke Z, Xie C, Zhou W. Dynamic evolution analysis of stock price fluctuation and its control. Complexity. 2018;2018:9 pages, Article ID 5728090.
27. Xu Y, Zhou W, Fang Ja, Xie C, Tong D. Finite-time synchronization of the complex dynamical network with non-derivative and derivative coupling. Neurocomputing. 2016;173:1356-61.
28. Majd VJ, Mobayen S. An ISM-based CNF tracking controller design for uncertain MIMO linear systems with multiple time-delays and external disturbances. Nonlinear Dynamics. 2015;80(1-2):591-613.
29. Cai L, Chen FY, Lu FF. Global robust sliding mode tracking control for helicopter with input time delay. Advanced Materials Research. 2014;846:434-7.
30. Shao K, Ma Q. Global fuzzy sliding mode control for multi-joint robot manipulators based on backstepping. Foundations of Intelligent Systems: Springer; 2014. p. 995-1004.
31. Zhong T, Yuanwei J, Chengyin Y, Nan J. Global sliding mode control based on observer for TCP network. The 26th Chinese Control and Decision Conference (2014 CCDC)2014. p. 4946-50.
32. Wu M, Chen J. A Discrete-Time Global Quasi-Sliding Mode Control Scheme with Bounded External Disturbance Rejection. Asian Journal of Control. 2014;16(6):1839-48.

33. Chen F, Jiang R, Wen C, Su R. Self-repairing control of a helicopter with input time delay via adaptive global sliding mode control and quantum logic. Information Sciences. 2015;316:123-31.
34. Mobayen S. An adaptive fast terminal sliding mode control combined with global sliding mode scheme for tracking control of uncertain nonlinear third-order systems. Nonlinear Dynamics. 2015;82(1-2):599-610.
35. Chu Y, Fei J. Adaptive global sliding mode control for MEMS gyroscope using RBF neural network. Mathematical Problems in Engineering. 2015;2015:9 pages, Article ID 403180.
36. Mobayen S, Baleanu D. Linear matrix inequalities design approach for robust stabilization of uncertain nonlinear systems with perturbation based on optimally-tuned global sliding mode control. Journal of Vibration and Control. 2017;23(8):1285-95.
37. Mobayen S, Baleanu D. Stability analysis and controller design for the performance improvement of disturbed nonlinear systems using adaptive global sliding mode control approach. Nonlinear Dynamics. 2016;83(3):1557-65.
38. Mobayen S. A novel global sliding mode control based on exponential reaching law for a class of underactuated systems with external disturbances. Journal of Computational and Nonlinear Dynamics. 2016;11(2):021011.
39. Chu Y, Fang Y, Fei J. Adaptive neural dynamic global PID sliding mode control for MEMS gyroscope. International Journal of Machine Learning and Cybernetics. 2017;8(5):1707-18.
40. Mobayen S, Tchier F, Ragoub L. Design of an adaptive tracker for n-link rigid robotic manipulators based on super-twisting global nonlinear sliding mode control. International Journal of Systems Science. 2017;48(9):1990-2002.
41. Xiu C, Hou J, Xu G, Zang Y. Improved fast global sliding mode control based on the exponential reaching law. Advances in Mechanical Engineering. 2017. doi: 10.1177/1687814016687967.
42. Sprott J, Jafari S, Pham V-T, Hosseini ZS. A chaotic system with a single unstable node. Physics Letters A. 2015;379(36):2030-6.
43. Kengne J, Njitacke Tabekoueng Z, Kamdoum Tamba V, Nguomkam Negou A. Periodicity, chaos, and multiple attractors in a memristor-based Shinriki's circuit. Chaos: An Interdisciplinary Journal of Nonlinear Science. 2015;25(10):103126.
44. Yuan F, Wang G, Wang X. Extreme multistability in a memristor-based multi-scroll hyper-chaotic system. Chaos: An Interdisciplinary Journal of Nonlinear Science. 2016;26(7):073107.
45. Wei Z, Moroz I, Sprott J, Akgul A, Zhang W. Hidden hyperchaos and electronic circuit application in a 5D self-exciting homopolar disc dynamo. Chaos: An Interdisciplinary Journal of Nonlinear Science. 2017;27(3):033101.
46. Lv M, Wang C, Ren G, Ma J, Song X. Model of electrical activity in a neuron under magnetic flow effect. Nonlinear Dynamics. 2016;85(3):1479-90.
47. Qin H, Ma J, Jin W, Wang C. Dynamics of electric activities in neuron and neurons of network induced by autapses. Science China Technological Sciences. 2014;57(5):936-46.